

## RESEARCH

# Molecular De-Novo Design through Deep Reinforcement Learning

Marcus Olivecrona<sup>\*</sup>, Thomas Blaschke<sup>†</sup>, Ola Engkvist<sup>†</sup> and Hongming Chen<sup>†</sup>**Abstract**

This work introduces a method to tune a sequence-based generative model for molecular *de novo* design that through augmented episodic likelihood can learn to generate structures with certain specified desirable properties. We demonstrate how this model can execute a range of tasks such as generating analogues to a query structure and generating compounds predicted to be active against a biological target. As a proof of principle, the model is first trained to generate molecules that do not contain sulphur. As a second example, the model is trained to generate analogues to the drug Celecoxib, a technique that could be used for scaffold hopping or library expansion starting from a single molecule. Finally, when tuning the model towards generating compounds predicted to be active against the dopamine receptor type 2, the model generates structures of which more than 95% are predicted to be active, including experimentally confirmed actives that have not been included in either the generative model nor the activity prediction model.

**Keywords:** *De Novo* design; Recurrent Neural Networks; Reinforcement Learning

## 1 Introduction

Drug discovery is often described using the metaphor of finding a needle in a haystack. In this case, the haystack comprises on the order of  $10^{60} - 10^{100}$  synthetically feasible molecules [1], out of which we need to find a compound which satisfies the plethora of criteria such as bioactivity, drug metabolism and pharmacokinetic (DMPK) profile, synthetic accessibility, etc. The fraction of this space that we can synthesize and test at all - let alone efficiently - is negligible. By using algorithms to virtually design and assess molecules, *de novo* design offers ways to reduce the chemical space into something more manageable for the search of the needle.

Early *de novo* design algorithms [1] used structure based approaches to grow ligands to sterically and electronically fit the binding pocket of the target of interest [2, 3]. A limitation of these methods is that the molecules created often possess poor DMPK properties and can be synthetically intractable. In contrast, the ligand based approach is to generate a large virtual library of chemical structures, and search this chemical space using a scoring function that typically takes

into account several properties such as DMPK profiles, synthetic accessibility, bioactivity, and query structure similarity [4, 5]. One way to create such a virtual library is to use known chemical reactions alongside a set of available chemical building blocks, resulting in a large number of synthetically accessible structures [6]; another possibility is to use transformational rules based on the expertise of medicinal chemists to design analogues to a query structure. For example, Besnard *et al.* [7] applied a transformation rule approach to the design of novel dopamine receptor type 2 (DRD2) receptor active compounds with specific polypharmacological profiles and appropriate DMPK profiles for a central nervous system indication. Although using either transformation or reaction rules can reliably and effectively generate novel structures, they are limited by the inherent rigidity and scope of the predefined rules and reactions.

A third approach, known as inverse Quantitative Structure Activity Relationship (inverse QSAR), tackles the problem from a different angle: rather than first generating a virtual library and then using a QSAR model to score and search this library, inverse QSAR aims to map a favourable region in terms of predicted activity to the corresponding molecular structures [8–10]. This is not a trivial problem: first the solutions of molecular descriptors corresponding to the region need to be resolved using the QSAR model, and these

<sup>\*</sup>Correspondence: [m.olivecrona@gmail.com](mailto:m.olivecrona@gmail.com)

Hit Discovery, Discovery Sciences, Innovative Medicines and Early Development Biotech Unit, AstraZeneca R&D Gothenburg, 43183 Mölndal, Sweden

Full list of author information is available at the end of the article

<sup>†</sup>[thomas.blaschke@astrazeneca.com](mailto:thomas.blaschke@astrazeneca.com), [ola.engkvist@astrazeneca.com](mailto:ola.engkvist@astrazeneca.com),

[hongming.chen@astrazeneca.com](mailto:hongming.chen@astrazeneca.com)

then need be mapped back to the corresponding molecular structures. The fact that the molecular descriptors chosen need to be suitable both for building a forward predictive QSAR model as well as for translation back to molecular structure is one of the major obstacles for this type of approach.

The Recurrent Neural Network (RNN) is commonly used as a generative model for data of sequential nature, and have been used successfully for tasks such as natural language processing [11] and music generation [12]. Recently, there has been an increasing interest in using this type of generative model for the *de novo* design of molecules [13–15]. By using a data-driven method that attempts to learn the underlying probability distribution over a large set of chemical structures, the search over the chemical space can be reduced to only molecules seen as reasonable, without introducing the rigidity of rule based approaches. Segler *et al.* demonstrated that an RNN trained on the canonicalized SMILES representation of molecules can learn both the syntax of the language as well as the distribution in chemical space [13]. They also show how further training of the model using a focused set of actives towards a biological target can produce a fine-tuned model which generates a high fraction of predicted actives.

In two recent studies, reinforcement learning (RL) [16] was used to fine tune pre-trained RNNs. Yu *et al.* [15] use an adversarial network to estimate the expected return for state-action pairs sampled from the RNN, and by increasing the likelihood of highly rated pairs improves the generative network for tasks such as poem generation. Jaques *et al.* [17] use Deep Q-learning to improve a pre-trained generative RNN by introducing two ways to score the sequences generated: one is a measure of how well the sequences adhere to music theory, and one is the likelihood of sequences according to the initial pre-trained RNN. Using this concept of prior likelihood they reduce the risk of forgetting what was initially learnt by the RNN, compared to a reward based only on the adherence to music theory. The authors demonstrate significant improvements over both the initial RNN as well as an RL only approach. They later extend this method to several other tasks including the generation of chemical structures, and optimize toward molecular properties such as cLogP [18] and QED drug-likeness [19]. However, they report that the method is dependent on a reward function incorporating handwritten rules to penalize undesirable types of sequences, and even then can lead to exploitation of the reward resulting in unrealistically simple molecules that are more likely to satisfy the optimization requirements than more complex structures [17].

In this study we propose a policy based RL approach to tune RNNs for episodic tasks [16], in this case the

task of generating molecules with given desirable properties. Through learning an augmented episodic likelihood which is a composite of prior likelihood [17] and a user defined scoring function, the method aims to fine-tune an RNN pre-trained on the ChEMBL database [20] towards generating desirable compounds. Compared to maximum likelihood estimation finetuning [13], this method can make use of negative as well as continuous scores, and may reduce the risk of catastrophic forgetting [21]. The method is applied to several different tasks of molecular *de novo* design, and an investigation was carried out to illustrate how the method affects the behaviour of the generative model on a mechanistic level.

## 2 Methods

### 2.1 Recurrent Neural Networks

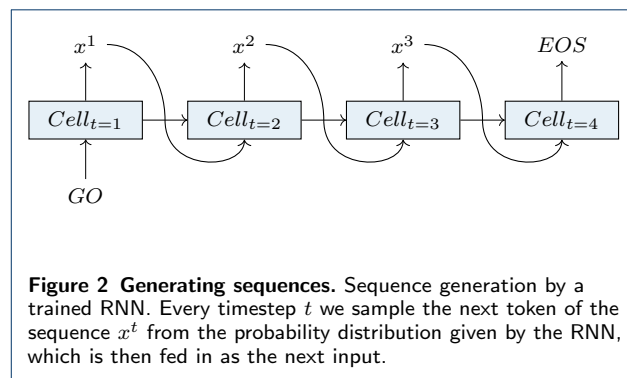
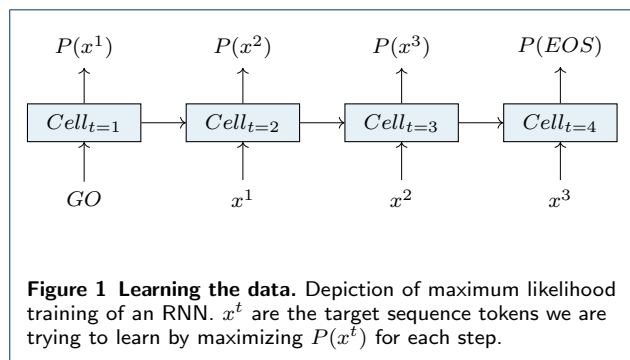
A recurrent neural network is an architecture of neural networks designed to make use of the symmetry across steps in sequential data while simultaneously at every step keeping track of the most salient information of previously seen steps, which may affect the interpretation of the current one [22]. It does so by introducing the concept of a *cell* (Figure 1). For any given step  $t$ , the  $cell_t$  is a result of the previous  $cell_{t-1}$  and the current input  $x^{t-1}$ . The content of  $cell_t$  will determine both the output at the current step as well as influence the next cell state. The cell thus enables the network to have a memory of past events, which can be used when deciding how to interpret new data. These properties make an RNN particularly well suited for problems in the domain of natural language processing. In this setting, a sequence of words can be encoded into one-hot vectors the length of our vocabulary  $X$ . Two additional tokens, *GO* and *EOS*, may be added to denote the beginning and end of the sequence respectively.

#### 2.1.1 Learning the data

Training an RNN for sequence modeling is typically done by maximum likelihood estimation of the next token  $x^t$  in the target sequence given tokens for the previous steps (Figure 1). At every step the model will produce a probability distribution over what the next character is likely to be, and the aim is to maximize the likelihood assigned to the correct token:

$$J(\Theta) = - \sum_{t=1}^T \log P(x^t | x^{t-1}, \dots, x^1)$$

The cost function  $J(\Theta)$ , often applied to a subset of all training examples known as a batch, is minimized with respect to the network parameters  $\Theta$ . Given a predicted log likelihood  $\log P$  of the target at step  $t$ , the gradient



of the prediction with respect to  $\Theta$  is used to make an update of  $\Theta$ . This method of fitting a neural network is called back-propagation. Due to the architecture of the RNN, changing the network parameters will not only affect the direct output at time  $t$ , but also affect the flow of information from the previous cell into the current one iteratively. This domino-like effect that the recurrence has on back-propagation gives rise to some particular problems, and back-propagation applied to RNNs is referred to as back-propagation through time (BPTT).

BPTT is dealing with gradients that through the chain-rule contains terms which are multiplied by themselves many times, and this can lead to a phenomenon known as exploding and vanishing gradients. If these terms are not unity, the gradients quickly become either very large or very small. In order to combat this issue, Hochreiter *et al.* introduced the Long-Short-Term Memory cell [23], which through a more controlled flow of information can decide what information to keep and what to discard. The Gated Recurrent Unit is a simplified implementation of the Long-Short-Term Memory architecture that achieves much of the same effect at a reduced computational cost [24].

### 2.1.2 Generating new samples

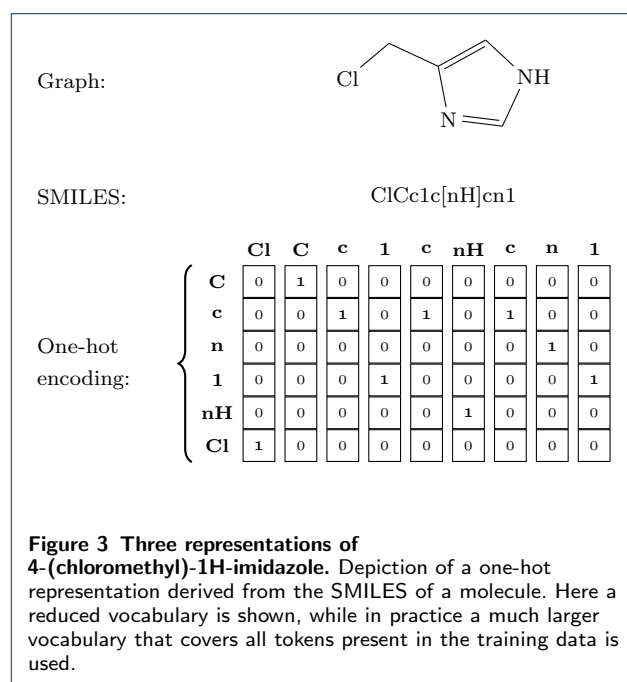
Once an RNN has been trained on target sequences, it can then be used to generate new sequences that follow the conditional probability distributions learned from the training set. The first input - the *GO* token - is given and at every timestep after we sample an output token  $x^t$  from the predicted probability distribution  $P(X^t)$  over our vocabulary  $X$  and use  $x^t$  as our next input. Once the *EOS* token is sampled, the sequence is considered finished (Figure 2).

### 2.1.3 Tokenizing and one-hot encoding SMILES

A SMILES [25] represents a molecule as a sequence of characters corresponding to atoms as well as special characters denoting opening and closure of rings and branches. The SMILES is, in most cases, tokenized

based on a single character, except for atom types which comprise two characters such as "Cl" and "Br" and special environments denoted by square brackets (e.g [nH]), where they are considered as one token. This method of tokenization resulted in 86 tokens present in the training data. Figure 3 exemplifies how a chemical structure is translated to both the SMILES and one-hot encoded representations.

There are many different ways to represent a single molecule using SMILES. Algorithms that always represent a certain molecule with the same SMILES are referred to as canonicalization algorithms [26]. However, different implementations of the algorithms can still produce different SMILES.



## 2.2 Reinforcement Learning

Consider an Agent, that given a certain state  $s \in \mathbb{S}$  has to choose which action  $a \in \mathbb{A}(s)$  to take, where  $\mathbb{S}$  is

the set of possible states and  $\mathbb{A}(s)$  is the set of possible actions for that state. The policy  $\pi(a | s)$  of an Agent maps a state to the probability of each action taken therein. Many problems in reinforcement learning are framed as Markov decision processes, which means that the current state contains all information necessary to guide our choice of action, and that nothing more is gained by also knowing the history of past states. For most real problems, this is an approximation rather than a truth; however, we can generalize this concept to that of a partially observable Markov decision process, in which the Agent can interact with an incomplete representation of the environment. Let  $r(a | s)$  be the reward which acts as a measurement of how good it was to take an action at a certain state, and the long-term return  $G(a_t, S_t = \sum_t^T r_t)$  as the cumulative rewards starting from  $t$  collected up to time  $T$ . Since molecular desirability in general is only sensible for a completed SMILES, we will refer only to the return of a complete sequence.

What reinforcement learning concerns, given a set of actions taken from some states and the rewards thus received, is how to improve the Agent policy in such a way as to increase the expected return  $\mathbb{E}[G]$ . A task which has a clear endpoint at step  $T$  is referred to as an episodic task [16], where  $T$  corresponds to the length of the episode. Generating a SMILES is an example of an episodic task, which ends once the *EOS* token is sampled.

The states and actions used to train the agent can be generated both by the agent itself or by some other means. If they are generated by the agent itself the learning is referred to as *on-policy*, and if they are generated by some other means the learning is referred to as *off-policy* [16].

There are two different approaches often used in reinforcement learning to obtain a policy: value based RL, and policy based RL [16]. In value based RL, the goal is to learn a value function that describes the expected return from a given state. Having learnt this function, a policy can be determined in such a way as to maximize the expected value of the state that a certain action will lead to. In policy based RL on the other hand, the goal is to directly learn a policy. For the problem addressed in this study, we believe that policy based methods is the natural choice for three reasons:

- Policy based methods can learn explicitly an optimal stochastic policy [16], which is our goal.
- The method used starts with a prior sequence model. The goal is to finetune this model according to some specified scoring function. Since the prior model already constitutes a policy, learning a finetuned policy might require only small changes to the prior model.

- The episodes in this case are short and fast to sample, reducing the impact of the variance in the estimate of the gradients.

In Section 3.4 the change in policy between the prior and the finetuned model is investigated, providing justification for the second point.

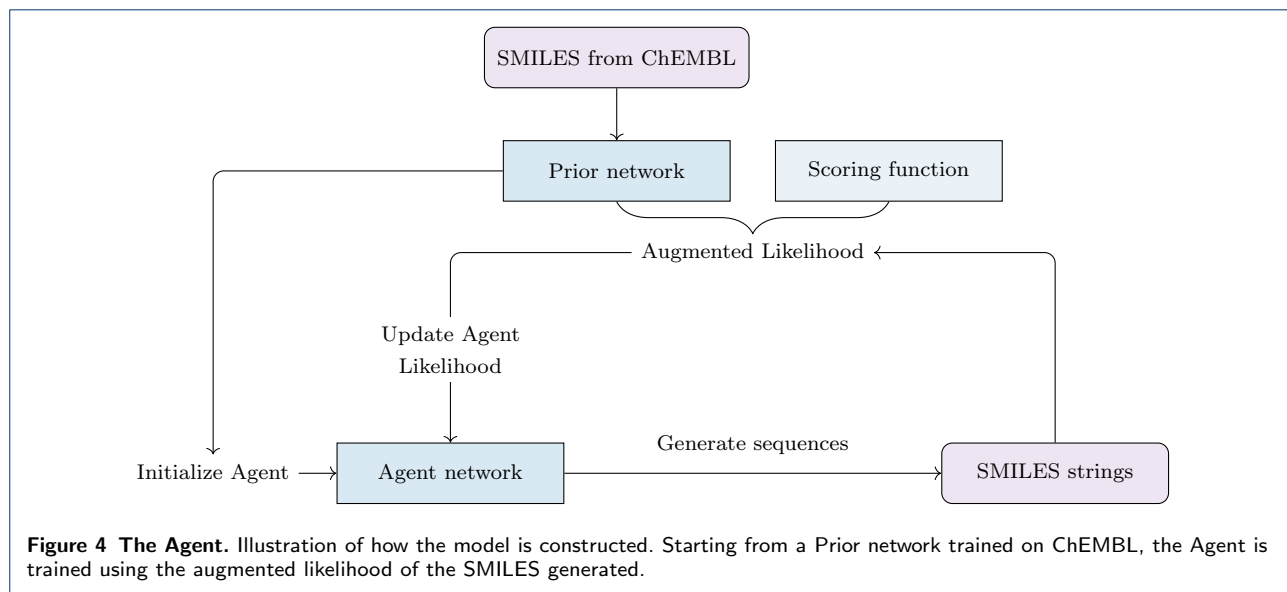
### 2.3 The Prior network

Maximum likelihood estimation was employed to train the initial RNN composed of 3 layers with 1024 Gated Recurrent Units (forget bias 5) in each layer. The RNN was trained on the RDKit [27] canonical SMILES of 1.5 million structures from ChEMBL [20] where the molecules were restrained to containing between 10 and 50 heavy atoms and elements  $\in \{H, B, C, N, O, F, Si, P, S, Cl, Br, I\}$ . The model was trained with stochastic gradient descent for 50 000 steps using a batch size of 128, utilizing the Adam optimizer [28] ( $\beta_1 = 0.9$ ,  $\beta_2 = 0.999$ , and  $\epsilon = 10^{-8}$ ) with an initial learning rate of 0.001 and a 0.02 learning rate decay every 100 steps. Gradients were clipped to  $[-3, 3]$ . Tensorflow [29] was used to implement the Prior as well as the RL Agent.

### 2.4 The Agent network

We now frame the problem of generating a SMILES representation of a molecule with specified desirable properties via an RNN as a partially observable Markov decision process, where the agent must make a decision of what character to choose next given the current cell state. We use the probability distributions learnt by the previously described prior model as our initial prior policy. We will refer to the network using the prior policy simply as the *Prior*, and the network whose policy has since been modified as the *Agent*. The Agent is thus also an RNN with the same architecture as the Prior. The task is episodic, starting with the first step of the RNN and ending when the *EOS* token is sampled. The sequence of actions  $A = a_1, a_2, \dots, a_T$  during this episode represents the SMILES generated and the product of the action probabilities  $P(A) = \prod_{t=1}^T \pi(a_t | s_t)$  represents the model likelihood of the sequence formed. Let  $S(A) \in [-1, 1]$  be a scoring function that rates the desirability of the sequences formed using some arbitrary method. The goal now is to update the agent policy  $\pi$  from the prior policy  $\pi_{Prior}$  in such a way as to increase the expected score for the generated sequences. However, we would like our new policy to be anchored to the prior policy, which has learnt both the syntax of SMILES and distribution of molecular structure in ChEMBL [13]. We therefore denote an augmented likelihood  $\log P(A)_{\mathbb{U}}$  as a prior likelihood modulated by the desirability of a sequence:

$$\log P(A)_{\mathbb{U}} = \log P(A)_{Prior} + \sigma S(A)$$



where  $\sigma$  is a scalar coefficient. The return  $G(A)$  of a sequence  $A$  can in this case be seen as the agreement between the Agent likelihood  $\log P(A)_{\mathbb{A}}$  and the augmented likelihood:

$$G(A) = -[\log P(A)_{\mathbb{U}} - \log P(A)_{\mathbb{A}}]^2$$

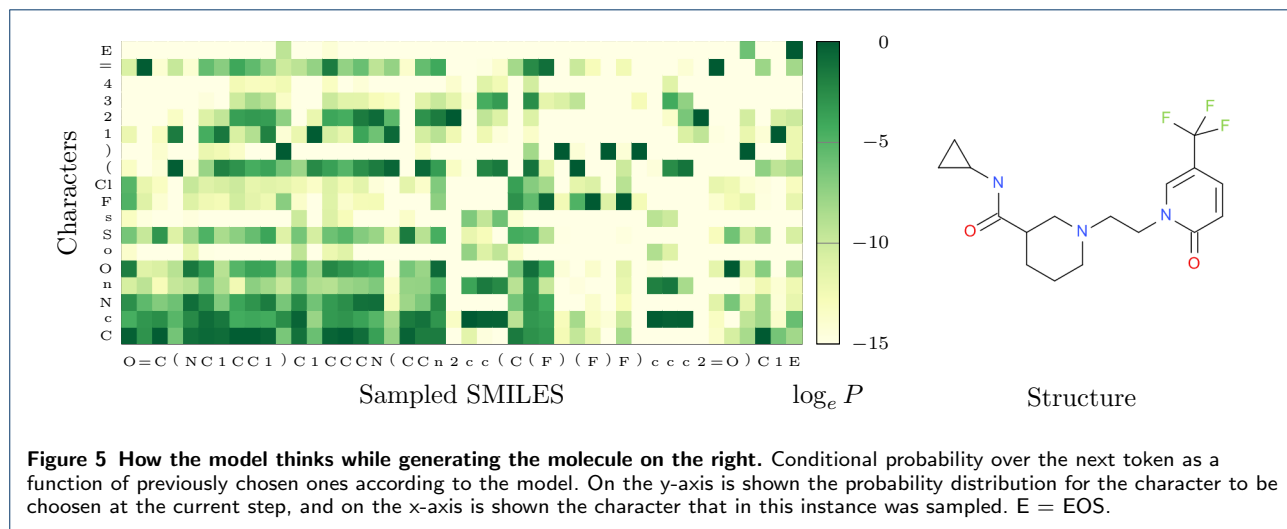
The goal of the Agent is to learn a policy which maximizes the expected return, achieved by minimizing the cost function  $L(\Theta) = -G$ . The fact that we describe the target policy using the policy of the Prior and the scoring function enables us to formulate this cost function. In the appendix we show how this approach can be described using a REINFORCE [30] algorithm with a final step reward of  $r(t) = [\log P(A)_{\mathbb{U}} - \log P(A)_{\mathbb{A}}]^2 / \log P(A)_{\mathbb{A}}$ . We believe this is a more natural approach to the problem than REINFORCE algorithms directly using rewards of  $S(A)$  or  $\log P(A)_{\text{Prior}} + \sigma S(A)$ . In Section 3.2 we compare our approach to these methods. The Agent is trained in an on-policy fashion on batches of 128 generated sequences, making an update to  $\pi$  after every batch has been generated and scored. A standard gradient descent optimizer with a learning rate of 0.0005 was used and gradients were clipped to  $[-3, 3]$ .

Figure 4 shows an illustration of how the Agent, initially identical to the Prior, is trained using reinforcement learning. The training shifts the probability distribution from that of the Prior towards a distribution modulated by the desirability of the structures. This method adopts a similar concept to Jaques *et al.* [17], while using a policy based RL method that introduces a novel cost function with the aim of addressing the need for handwritten rules and the issues of generating structures that are too simple.

In all the tasks investigated below, the scoring function is fixed during the training of the Agent. If instead the scoring function used is defined by a discriminator network whose task is to distinguish sequences generated by the Agent from ‘real’ SMILES (e.g. a set of actives), the method could be described as a type of Generative Adversarial Network [31], where the Agent and the discriminator would be jointly trained in a game where they both strive to beat the other. This is the approach taken by Yu *et al.* [15] to fine-tune a pretrained sequence model for poem generation. Guimaraes *et al.* demonstrates how such a method can be combined with a fixed scoring function for molecular *de novo* design [32].

## 2.5 The DRD2 activity model

In one of our studies the objective of the Agent is to generate molecules that are predicted to be active against a biological target. The dopamine type 2 receptor DRD2 was chosen as the target, and corresponding bioactivity data was extracted from ExCAPE-DB [33]. In this dataset there are 7218 actives ( $\text{pIC}_{50} > 5$ ) and 343204 inactives ( $\text{pIC}_{50} < 5$ ). A subset of 100 000 inactive compounds was randomly selected. In order to decrease the nearest neighbour similarity between the training and testing structures [34–36], the actives were grouped in clusters based on their molecular similarity. The Jaccard [37] index, for binary vectors also known as the Tanimoto similarity, based on the RDKit implementation of binary Extended Connectivity Molecular Fingerprints with a diameter of 6 (ECFP6 [38]) was used as a similarity measure and the actives were clustered using the Butina clustering algorithm [39] in RDKit with a clustering cutoff of 0.4. In this algorithm,



centroid molecules will be selected, and everything with a similarity higher than 0.4 to these centroids will be assigned to the same cluster. The centroids are chosen such as to maximize the number of molecules that are assigned to any cluster. The clusters were sorted by size and iteratively assigned to the test, validation, and training sets (assigned 4 clusters each iteration) to give a distribution of  $\frac{1}{6}$ ,  $\frac{1}{6}$ , and  $\frac{4}{6}$  of the clusters respectively. The inactive compounds, of which less than 0.5% were found to belong to any of the clusters formed by the actives, were split randomly into the three sets using the same ratios.

A support vector machine (SVM) classifier with a Gaussian kernel was built in Scikit-learn [40] on the training set as a predictive model for DRD2 activity. The optimal C and Gamma values utilized in the final model were obtained from a grid search for the highest ROC-AUC performance on the validation set.

### 3 Results and Discussion

#### 3.1 Structure generation by the Prior

After the initial training, 94% of the sequences generated by the Prior as described in Section 2.1.2 corresponded to valid molecular structures according to RDKit [27] parsing, out of which 90% are novel structures outside of the training set. A set of randomly chosen structures generated by the Prior, as well as by Agents trained in the subsequent examples, are shown in the appendix. The process of generating a SMILES by the Prior is illustrated in Figure 5. For every token in the generated SMILES sequence, the conditional probability distribution over the vocabulary at this step according to the Prior is displayed. The sequence of distributions are depicted in Figure 5. For the first step, when no information other than the initial GO token is present, the distribution is an approximation

of the distribution of first tokens for the SMILES in the ChEMBL training set. In this case "O" was sampled, but "C", "N", and the halogens were all likely as well. Corresponding log likelihoods were -0.3 for "C", -2.7 for "N", -1.8 for "O", and -5.0 for "F" and "Cl".

A few (unsurprising) observations:

- Once the aromatic "n" has been sampled, the model has come to expect a ring opening (i.e. a number), since aromatic moieties by definition are cyclic.
- Once an aromatic ring has been opened, the aromatic atoms "c", "n", "o", and "s" become probable, until 5 or 6 steps later when the model thinks it is time to close the ring.
- The model has learnt the RDKit canonicalized SMILES format of increasing ring numbers, and expects the first ring to be numbered "1". Ring numbers can be reused, as in the two first rings in this example. Only once "1" has been sampled does it expect a ring to be numbered "2" and so on.

#### 3.2 Learning to avoid sulphur

As a proof of principle the Agent was first trained to generate molecules which do not contain sulphur. The method described in Section 2.4 is compared with three other policy gradient based methods. The first alternative method is the same as the Agent method, with the only difference that the loss is defined on an action basis rather than on an episodic one, resulting in the cost function:

$$J(\Theta) = \left[ \sum_{t=0}^T (\log \pi_{Prior}(a_t, s_t) - \log \pi_{\Theta}(a_t, s_t)) + \sigma S(A) \right]^2$$

We refer to this method as 'Action basis'. The second alternative is a REINFORCE algorithm with a reward

**Table 1** Comparison of model performance and properties for non-sulphur containing structures generated by the two models. Properties reported as Mean  $\pm$  StdDev.

Model	Prior	Agent	Action basis	REINFORCE	REINFORCE + Prior
Fraction of valid SMILES	0.94 $\pm$ 0.01	0.95 $\pm$ 0.01	0.95 $\pm$ 0.01	0.98 $\pm$ 0.00	0.98 $\pm$ 0.00
Fraction without sulphur	0.66 $\pm$ 0.01	0.98 $\pm$ 0.00	0.92 $\pm$ 0.02	0.98 $\pm$ 0.00	0.92 $\pm$ 0.01
Average molecular weight	371 $\pm$ 1.70	367 $\pm$ 3.30	372 $\pm$ 0.94	585 $\pm$ 27.4	232 $\pm$ 5.25
Average cLogP	3.36 $\pm$ 0.04	3.37 $\pm$ 0.09	3.39 $\pm$ 0.02	11.3 $\pm$ 0.85	3.05 $\pm$ 0.02
Average NumRotBonds	5.39 $\pm$ 0.04	5.41 $\pm$ 0.07	6.08 $\pm$ 0.04	30.0 $\pm$ 2.17	2.8 $\pm$ 0.11
Average NumAromRings	2.26 $\pm$ 0.02	2.26 $\pm$ 0.02	2.09 $\pm$ 0.02	0.57 $\pm$ 0.04	2.11 $\pm$ 0.02

**Table 2** Randomly selected SMILES generated by the different models.

Model	Sampled SMILES
Prior	CCOC(=O)C1=C(C)OC(N)=C(C#N)C1c1cccc1C(F)(F)F COC(=O)CC(C)=NNc1ccc(N(C)C)cc1[N+](=O)[O-] Cc1cccc1CNS(=O)(=O)c1ccc2c(c1)C(=O)C(=O)N2
Agent	CC(C)(C)NC(=O)c1ccc(OCc2cccc2C(F)(F)F)nc1-c1cccc1 CC(=O)NCC1OC(=O)N2c3ccc(-c4cccnc4)cc3OCC12 OCCCNc1cccc(-c2cccc(-c3nc4cccc4[nH]3)c2OCCOc2ncc(Cl)cc2Br)c1
Action level	CCN1CC(C)(C)OC(=O)c2cc(-c3ccc(Cl)cc3)ccc21 CCC(CC)C(=O)Nc1ccc2cnn(-c3ccc(C(C)=O)cc3)c2c1 CCCCN1C(=O)c2cccc2NC1c1ccc(OC)cc1
REINFORCE	CC1CCCCC12NC(=O)N(CC(=O)Nc1cccc1C(=O)O)C2=O CCCCCCCCCCCCCCCCCCCCCCCCCCCCCCCCCNC(=O)OCCCCC CCCCCCCCCCCCCCCCCCCCCCCCCCCCCCCCC1CCC(O)C1(CCC)CCCCCCCCCCCCC
REINFORCE + Prior	Nc1cccc1C(=O)Oc1cccc1 O=c1cccc1Oc1cccc1 Nc1ccc(-c2cccc2O)cc1

of  $S(A)$  given at the last step. This method is similar to the one used by Silver *et al.* to train the policy network in AlphaGo [41], as well as the method used by Yu *et al.* [15]. We refer to this method as ‘REINFORCE’. The corresponding cost function can be written as:

$$J(\Theta) = S(A) \sum_{t=0}^T \log \pi_{\Theta}(a_t, s_t)$$

A variation of this method that considers prior likelihood is defined by changing the reward from  $S(A)$  to  $S(A) + \log P(A)_{Prior}$ . This method is referred to as ‘REINFORCE + Prior’, with the cost function:

$$J(\Theta) = [\log P(A)_{Prior} + \sigma S(A)] \sum_{t=0}^T \log \pi_{\Theta}(a_t, s_t)$$

Note that the last method by nature strives to generate only the putative sequence with the highest reward. In contrast to the Agent, the optimal policy for this method is not stochastic. This tendency could be restrained by introducing a regularizing policy entropy term. However, it was found that such regularization undermined the models ability to produce valid SMILES. This method is therefore dependent on only training sufficiently long for the model to reach a point where highly scored sequences are generated, without being

settled in a local minima. The experiment aims to answer the following questions:

- Can the models achieve the task of generating valid SMILES corresponding to structures that do not contain sulphur?
- Will the models exploit the reward function by converging on naïve solutions such as ‘C’ if not imposed handwritten rules?
- Are the distributions of physical chemical properties for the generated structures similar to those of sulphur free structures generated by the Prior?

The task is defined by the following scoring function:

$$S(A) = \begin{cases} 1 & \text{if valid and no S} \\ 0 & \text{if not valid} \\ -1 & \text{if contains S} \end{cases}$$

All the models were trained for 1000 steps starting from the Prior and 12800 SMILES sequences were sampled from all the models as well as the Prior. A learning rate of 0.0005 was used for the Agent and Action basis methods, and 0.0001 for the two REINFORCE methods. The values of  $\sigma$  used were 2 for the Agent and ‘REINFORCE + Prior’, and 8 for ‘Action basis’. To explore what effect the training has on the structures generated, relevant properties for non sulphur containing structures generated by both the Prior and the

other models were compared. The molecular weight, cLogP, the number of rotatable bonds, and the number of aromatic rings were all calculated using RDKit. The experiment was repeated three times with different random seeds. The results are shown in Table 1 and randomly selected SMILES generated by the Prior and the different models can be seen in Table 2. For the 'REINFORCE' method, where the sole aim is to generate valid SMILES that do not contain sulphur, the model quickly learns to exploit the reward function by generating sequences containing predominately 'C'. This is not surprising, since any sequence consisting only of this token always gets rewarded. For the 'REINFORCE + Prior' method, the inclusion of the prior likelihood in the reward function means that this is no longer a viable strategy (the sequences would be given a low prior probability). The model instead tries to find the structure with the best combination of score and prior likelihood, but as is evident from the SMILES generated and the statistics shown in Table 1, this results in small, simplistic structures being generated. Thus, both REINFORCE algorithms managed to achieve high scores according to the scoring function, but poorly represented the Prior. Both the Agent and the 'Action basis' methods have explicitly specified target policies. For the 'Action basis' method the policy is specified exactly on a stepwise level, while for the Agent the target policy is only specified to the likelihoods of entire sequences. Although the 'Action basis' method generates structures that are more similar to the Prior than the two REINFORCE methods, it performed worse than the Agent despite the higher value of  $\sigma$  used while also being slower to learn. This may be due to the less restricted target policy of the Agent, which could facilitate optimization. The Agent achieved the same fraction of sulphur free structures as the REINFORCE algorithms, while seemingly doing a much better job of representing the Prior. This is indicated by the similarity of the properties of the generated structures shown in Table 1 as well as the SMILES themselves shown in Table 2.

### 3.3 Similarity guided structure generation

The second task investigated was that of generating structures similar to a query structure. The Jaccard index [37]  $J_{i,j}$  of the RDKit implementation of FCFP4 [38] fingerprints was used as a similarity measure between molecules  $i$  and  $j$ . Compared to the DRD2 activity model (Section 2.5), the feature invariant version of the fingerprints and the smaller diameter 4 was used in order to get a more fuzzy similarity measure. The scoring function was defined as:

$$S(A) = -1 + 2 \times \frac{\min\{J_{i,j}, k\}}{k}$$

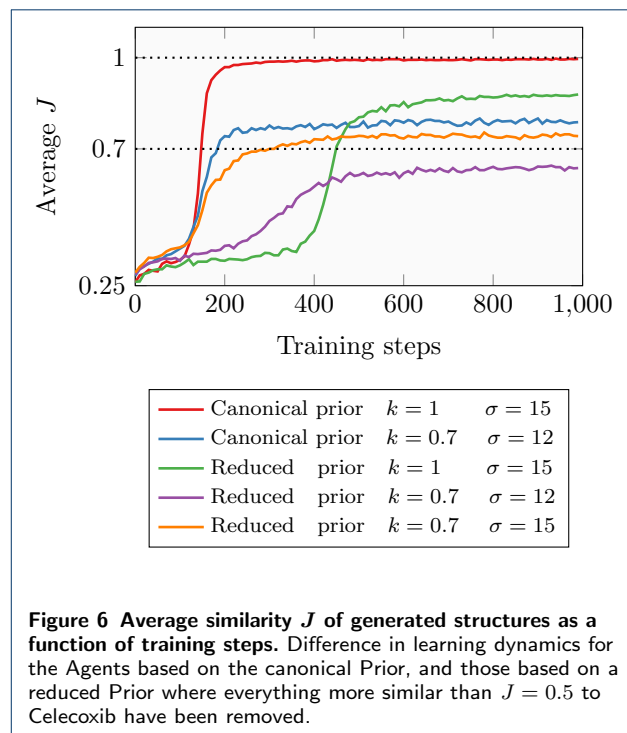
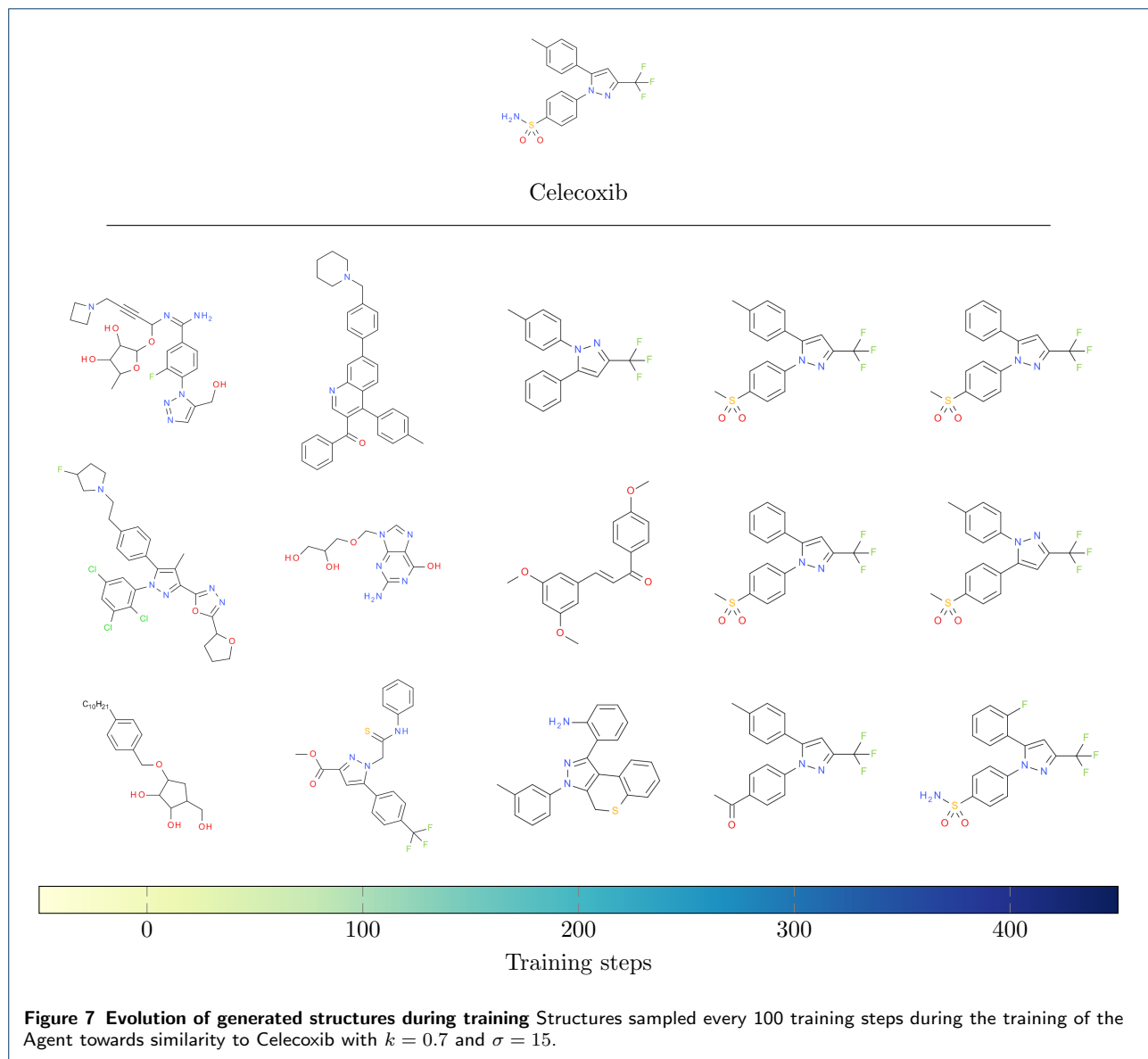


**Figure 6** Average similarity  $J$  of generated structures as a function of training steps. Difference in learning dynamics for the Agents based on the canonical Prior, and those based on a reduced Prior where everything more similar than  $J = 0.5$  to Celecoxib have been removed.

This definition means that an increase in similarity is only rewarded up to the point of  $k \in [0, 1]$ , as well as scaling the reward from  $-1$  (no overlap in the fingerprints between query and generated structure) to  $1$  (at least  $k$  degree of overlap). Celecoxib was chosen as our query structure, and we first investigated whether Celecoxib itself could be generated by using the high values of  $k = 1$  and  $\sigma = 15$ . The Agent was trained for 1000 steps. After a 100 training steps the Agent starts to generate Celecoxib, and after 200 steps it predominately generates this structure (Figure 6).

Celecoxib itself as well as many other similar structures appear in the ChEMBL training set used to build the Prior. An interesting question is whether the Agent could succeed in generating Celecoxib when these structures are not part of the chemical space covered by the Prior. To investigate this, all structures with a similarity to Celecoxib higher than 0.5 (corresponding to 1804 molecules) were removed from the training set and a new reduced Prior was trained. The prior likelihood of Celecoxib for the canonical and reduced Priors was compared, as well as the ability of the models to generate structures similar to Celecoxib. As expected, the prior probability of Celecoxib decreased when similar compounds were removed from the training set from  $\log_e P = -12.7$  to  $\log_e P = -19.2$ , representing a reduction in likelihood of a factor of 700. An Agent was then trained using the same hyperparameters as before, but on the reduced Prior. After 400 steps, the Agent again managed to find Celecoxib, albeit requiring more



time to do so. After 1000 steps, Celecoxib was the most commonly generated structure (about a third of the generated structures), followed by demethylated Celecoxib (also a third) whose SMILES is more likely according to the Prior with  $\log_e P = -15.2$  but has a lower similarity ( $J = 0.87$ ), resulting in an augmented likelihood equal to that of Celecoxib.

These experiments demonstrate that the Agent can be optimized using fingerprint based Jaccard similarity as the objective, but making copies of the query structure is hardly useful. A more useful example is that of generating structures that are moderately to the query structure. The Agent was therefore trained for 3000 steps, starting from both the canonical as well as the reduced Prior, using  $k = 0.7$  and  $\sigma = 12$ . The Agents

based on the canonical Prior quickly converge to their targets, while the Agents based on the reduced Prior converged more slowly. For the Agent based on the reduced Prior where  $k = 1$ , the fact that Celecoxib and demethylated Celecoxib are given similar augmented likelihoods means that the average similarity converges to around 0.9 rather than 1.0. For the Agent based on the reduced Prior where  $k = 0.7$ , the lower prior likelihood of compounds similar to Celecoxib translates to a lower augmented likelihood, which lowers the average similarity of the structures generated by the Agent.

To explore whether this reduced prior likelihood could be offset with a higher value of  $\sigma$ , an Agent starting from the reduced Prior was trained using  $\sigma = 15$ . Though taking slightly more time to converge than the

Agent based on the canonical Prior, this Agent too could converge to the target similarity. The learning curves for the different model is shown in Figure 6.

An illustration of how the type of structures generated by the Agent evolves during training is shown in Figure 7. For the Agent based on the reduced Prior with  $k = 0.7$  and  $\sigma = 15$ , three structures were randomly sampled every 100 training steps from step 0 up to step 400. At first, the structures are not similar to Celecoxib. After 200 steps, some features from Celecoxib have started to emerge, and after 300 steps the model generates mostly close analogues of Celecoxib.

We have investigated how various factors affect the learning behaviour of the Agent. In real drug discovery applications, we might be more interested in finding structures with modest similarity to our query molecules rather than very close analogues. For example, one of the structures sampled after 200 steps shown in Figure 7 displays a type of scaffold hopping where the sulphur functional group on one of the outer aromatic rings has been fused to the central pyrazole. The similarity to Celecoxib of this structure is 0.4, which may be a more interesting solution for scaffold-hopping purposes. One can choose hyperparameters and similarity criterion tailored to the desired output. Other types of similarity measures such as pharmacophoric fingerprints [42], Tversky substructure similarity [43], or presence/absence of certain pharmacophores could also be explored.

### 3.4 Target activity guided structure generation

The third example, perhaps the one most interesting and relevant for drug discovery, is to optimize the Agent towards generating structures with predicted biological activity. This can be seen as a form of inverse QSAR, where the Agent is used to implicitly map high predicted probability of activity to molecular structure. DRD2 was chosen as the biological target. The clustering split of the DRD2 activity dataset as described in Section 2.5 resulted in 1405, 1287, and 4526 actives in the test, validation, and training sets respectively. The average similarity to the nearest neighbour in the training set for the test set compounds was 0.53. For a random split of actives in sets of the same sizes this similarity was 0.69, indicating that the clustering had significantly decreased training-test set similarity which mimics the hit finding practice in drug discovery to identify diverse hits to the training set. Most of the DRD2 actives are also included in the ChEMBL dataset used to train the Prior. To explore the effect of not having the known actives included in the Prior, a reduced Prior was trained on a reduced subset of the ChEMBL training set where all DRD2 actives had been removed.

The optimal hyperparameters found for the SVM activity model were  $C = 2^7$ ,  $\gamma = 2^{-6}$ , resulting in a

**Table 3** Performance of the DRD2 activity model

Set	Training	Validation	Test
Accuracy	1.00	0.98	0.98
ROC-AUC	1.00	0.99	1.00
Precision	1.00	0.96	0.97
Recall	1.00	0.73	0.82

model whose performance is shown in Table 3. The good performance in general can be explained by the apparent difference between actives and inactive compounds as seen during the clustering, and the better performance on the test set compared to the validation set could be due to slightly higher nearest neighbour similarity to the training actives (0.53 for test actives and 0.48 for validation actives).

The output of the DRD2 model for a given structure is an uncalibrated predicted probability of being active  $P_{active}$ . This value is used to formulate the following scoring function:

$$S(A) = -1 + 2 \times P_{active}$$

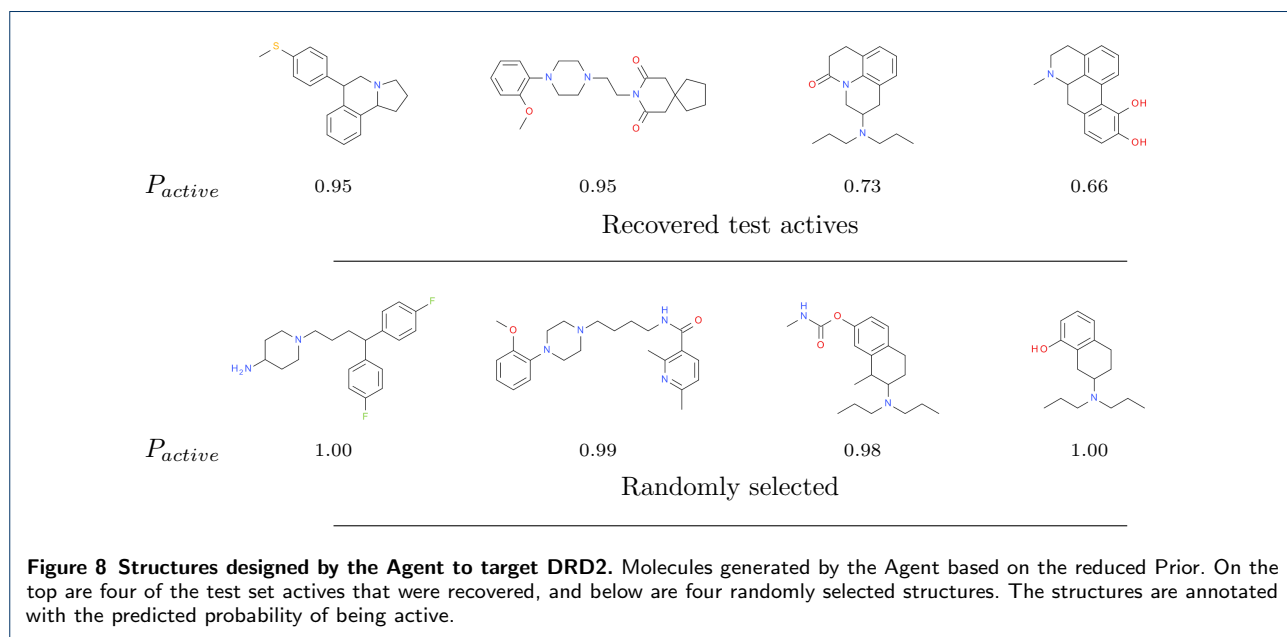
The model was trained for 3000 steps using  $\sigma = 7$ . After training, the fraction of predicted actives according to the DRD2 model increased from 0.02 for structures generated by the reduced Prior to 0.96 for structures generated by the corresponding Agent network (Table 4). To see how well the structure-activity-relationship learnt by the activity model is transferred to the type of structures generated by the Agent RNN, the fraction of compounds with an ECFP6 Jaccard similarity greater than 0.4 to any active in the training and test sets was calculated.

In some cases, the model recovered exact matches from the training and test sets (c.f. Segler *et al.* [13]). The fraction of recovered test actives recovered by the canonical and reduced Prior were 1.3% and 0.3% respectively. The Agent derived from the canonical Prior managed to recover 13% test actives; the Agent derived from the reduced Prior recovered 7%. For the Agent derived from the reduced Prior, where the DRD2 actives were excluded from the Prior training set, this means that the model has learnt to generate "novel" structures that have been seen neither by the DRD2 activity model nor the Prior, and are experimentally confirmed actives. We can formalize this observation by calculating the probability of a given generated sequence belonging to the set of test actives. For the canonical and reduced Priors, this probability was  $0.17 \times 10^{-3}$  and  $0.05 \times 10^{-3}$  respectively. Removing the actives from the Prior thus resulted in a threefold reduction in the probability of generating a structure from the set of test actives. For the Agents, the probabilities rose to  $15.0 \times 10^{-3}$  and  $40.2 \times 10^{-3}$  respectively, corresponding

**Table 4** Comparison of properties for structures generated by the canonical Prior, the reduced Prior, and corresponding Agents.

Model	Prior	Agent	Prior <sup>†</sup>	Agent <sup>†</sup>
Fraction valid SMILES	0.94	0.99	0.94	0.99
Fraction predicted actives	0.03	0.97	0.02	0.96
Fraction similar to train active	0.02	0.79	0.02	0.75
Fraction similar to test active	0.01	0.46	0.01	0.38
Fraction of test actives recovered ( $\times 10^{-3}$ )	13.5	126	2.85	72.6
Probability of generating a test set active ( $\times 10^{-3}$ )	0.17	40.2	0.05	15.0

<sup>†</sup>DRD2 actives withheld from the training of the Prior



to an enrichment of a factor of 250 over the Prior models. Again the consequence of removing the actives from the Prior was a threefold reduction in the probability of generating a test set active: the difference between the two Priors is directly mirrored by their corresponding Agents. Apart from generating a higher fraction of structures that are predicted to be active, both Agents also generate a significantly higher fraction of valid SMILES (Table 4). Sequences that are not valid SMILES receive a score of -1, which means that the scoring function naturally encourages valid SMILES.

A few of the test set actives generated by the Agent based on the reduced Prior along with a few randomly selected generated structures are shown together with their predicted probability of activity in Figure 8. Encouragingly, the recovered test set actives vary considerably in their structure, which would not have been the case had the Agent converged to generating only a certain type of very similar predicted active compounds.

Removing the known actives from the training set of the Prior resulted in an Agent which shows a decrease

in all metrics measuring the overlap between the known actives and the structures generated, compared to the Agent derived from the canonical Prior. Interestingly, the fraction of predicted actives did not change significantly. This indicates that the Agent derived from the reduced Prior has managed to find a similar chemical space to that of the canonical Agent, with structures that are equally likely to be predicted as active, but are less similar to the known actives. Whether or not these compounds are active will be dependent on the accuracy of the target activity model. Ideally, any predictive model to be used in conjunction with the generative model should cover a broad chemical space within its domain of applicability, since it initially has to assess representative structures of the dataset used to build the Prior [13].

Figure 9 shows a comparison of the conditional probability distributions for the reduced Prior and its corresponding Agent when a molecule from the set of test actives is generated. It can be seen that the changes are not drastic with most of the trends learnt by the Prior being carried over to the Agent. However, a big change in the probability distribution even only at



**Declarations**

Ethics approval and consent to participate  
Not applicable.

Consent for publication  
Not applicable.

**List of abbreviations**

- DMPK - Drug metabolism and pharmacokinetics
- DRD2 - Dopamine receptor D2
- QSAR - Quantitative structure activity relationship
- RNN - Recurrent neural network
- RL - Reinforcement Learning
- Log - Natural logarithm
- BPTT - Back-propagation through time
- *A* - Sequence of tokens constituting a SMILES
- Prior - An RNN trained on SMILES from ChEMBL used as a starting point for the Agent
- Agent - An RNN derived from a Prior, trained using reinforcement learning
- *J* - Jaccard index
- ECFP6 - Extended Molecular Fingerprints with diameter 6
- SVM - Support Vector Machine
- FCFP4 - Extended Molecular Fingerprints with diameter 4 and feature invariants

**Competing interests**

The authors declare that they have no competing interests.

**Funding**

MO, HC, and OE are employed by AstraZeneca. TB has received funding from the European Union's Horizon 2020 research and innovation program under the Marie Skłodowska-Curie grant agreement No 676434, "Big Data in Chemistry" ("BIGCHEM", <http://bigchem.eu>). The article reflects only the authors' view and neither the European Commission nor the Research Executive Agency (REA) are responsible for any use that may be made of the information it contains.

**Author's contributions**

MO contributed concept and implementation. All authors co-designed experiments. All authors contributed to the interpretation of results. MO wrote the manuscript. HC, TB, and OE reviewed and edited the manuscript. All authors read and approved the final manuscript.

**Acknowledgements**

The authors thank Thierry Kogej and Christian Tyrchan for general assistance and discussion, and Dominik Peters for his expertise in L<sup>A</sup>T<sub>E</sub>X.

**References**

1. Schneider, G., Fechner, U.: Computer-based de novo design of drug-like molecules. *Nat Rev Drug Discov* **4**(8), 649–663 (2005). doi:[10.1038/nrd1799](https://doi.org/10.1038/nrd1799)
2. Böhm, H.-J.: The computer program ludi: A new method for the de novo design of enzyme inhibitors. *Journal of Computer-Aided Molecular Design* **6**(1), 61–78 (1992). doi:[10.1007/BF00124387](https://doi.org/10.1007/BF00124387)
3. Gillet, V.J., Newell, W., Mata, P., Myatt, G., Sike, S., Zsoldos, Z., Johnson, A.P.: Sprout: Recent developments in the de novo design of molecules. *Journal of Chemical Information and Computer Sciences* **34**(1), 207–217 (1994). doi:[10.1021/ci00017a027](https://doi.org/10.1021/ci00017a027)
4. Ruedigkeit, L., Blum, L.C., Raymond, J.-L.: Visualization and virtual screening of the chemical universe database gdb-17. *Journal of Chemical Information and Modeling* **53**(1), 56–65 (2013). doi:[10.1021/ci300535x](https://doi.org/10.1021/ci300535x)
5. Hartenfeller, M., Zettl, H., Walter, M., Rupp, M., Reisen, F., Proschak, E., Weggen, S., Stark, H., Schneider, G.: Dogs: Reaction-driven de novo design of bioactive compounds. *PLOS Computational Biology* **8**, 1–12 (2012). doi:[10.1371/journal.pcbi.1002380](https://doi.org/10.1371/journal.pcbi.1002380)
6. Schneider, G., Geppert, T., Hartenfeller, M., Reisen, F., Klenner, A., Reutlinger, M., Hähne, V., Hiss, J.A., Zettl, H., Keppner, S., Spänkuch, B., Schneider, P.: Reaction-driven de novo design, synthesis and testing of potential type ii kinase inhibitors. *Future Medicinal Chemistry* **3**(4), 415–424 (2011). doi:[10.4155/fmc.11.8](https://doi.org/10.4155/fmc.11.8)
7. Besnard, J., Ruda, G.F., Setola, V., Abecassis, K., Rodriguiz, R.M., Huang, X.-P., Norval, S., Sassano, M.F., Shin, A.I., Webster, L.A., Simeons, F.R.C., Stojanovski, L., Prat, A., Seidah, N.G., Constam, D.B., Bickerton, G.R., Read, K.D., Wetsel, W.C., Gilbert, I.H., Roth, B.L., Hopkins, A.L.: Automated design of ligands to polypharmacological profiles. *Nature* **492**(7428), 215–220 (2012). doi:[10.1038/nature11691](https://doi.org/10.1038/nature11691)
8. Miyao, T., Kaneko, H., Funatsu, K.: Inverse qspr/qsar analysis for chemical structure generation (from y to x). *Journal of Chemical Information and Modeling* **56**(2), 286–299 (2016). doi:[10.1021/acs.jcim.5b00628](https://doi.org/10.1021/acs.jcim.5b00628)
9. Churchwell, C.J., Rintoul, M.D., Martin, S., Jr., D.P.V., Kotu, A., Larson, R.S., Sillerud, L.O., Brown, D.C., Faulon, J.-L.: The signature molecular descriptor: 3. inverse-quantitative structure–activity relationship of icam-1 inhibitory peptides. *Journal of Molecular Graphics and Modelling* **22**(4), 263–273 (2004). doi:[10.1016/j.jmgm.2003.10.002](https://doi.org/10.1016/j.jmgm.2003.10.002)
10. Wong, W.W., Burkowski, F.J.: A constructive approach for discovering new drug leads: Using a kernel methodology for the inverse-qsar problem. *J Cheminform* **1**, 4–4 (2009). doi:[10.1186/1758-2946-1-4](https://doi.org/10.1186/1758-2946-1-4)
11. Mikolov, T., Karafiát, M., Burget, L., Cernocký, J., Khudanpur, S.: Recurrent neural network based language model. In: *Interspeech*, vol. 2, p. 3 (2010)
12. Eck, D., Schmidhuber, J.: A first look at music composition using lstm recurrent neural networks. Technical report, Istituto Dalle Molle Di Studi Sull Intelligenza Artificiale (2002)
13. Segler, M.H.S., Kogej, T., Tyrchan, C., Waller, M.P.: Generating Focussed Molecule Libraries for Drug Discovery with Recurrent Neural Networks. *ArXiv e-prints* (2017). [1701.01329](https://arxiv.org/abs/1701.01329)
14. Gómez-Bombarelli, R., Duvenaud, D.K., Hernández-Lobato, J.M., Aguilera-Iparraguirre, J., Hirzel, T.D., Adams, R.P., Aspuru-Guzik, A.: Automatic chemical design using a data-driven continuous representation of molecules. *CoRR abs/1610.02415* (2016)
15. Yu, L., Zhang, W., Wang, J., Yu, Y.: Seqgan: Sequence generative adversarial nets with policy gradient. *CoRR abs/1609.05473* (2016)
16. Sutton, R., Barto, A.: *Reinforcement Learning: An Introduction*, 1st edn. MIT Press, Cambridge, MA (1998)
17. Jaques, N., Gu, S., Turner, R.E., Eck, D.: Tuning recurrent neural networks with reinforcement learning. *CoRR abs/1611.02796* (2016)
18. Leo, A., Hansch, C., Elkins, D.: Partition coefficients and their uses. *Chemical Reviews* **71**(6), 525–616 (1971). doi:[10.1021/cr60274a001](https://doi.org/10.1021/cr60274a001)
19. Bickerton, G.R., Paolini, G.V., Besnard, J., Muresan, S., Hopkins, A.L.: Quantifying the chemical beauty of drugs. *Nature Chemistry* **4**, 90–98 (2012). doi:[10.1038/nchem.1243](https://doi.org/10.1038/nchem.1243)
20. Gaulton, A., Bellis, L.J., Bento, A.P., Chambers, J., Davies, M., Hersey, A., Light, Y., McGlinchey, S., Michalovich, D., Al-Lazikani, B., Overington, J.P.: ChEMBL: a large-scale bioactivity database for drug discovery. *Nucleic Acids Res* **40**, 1100–1107 (2012). doi:[10.1093/nar/gkr777](https://doi.org/10.1093/nar/gkr777). Version 22
21. Goodfellow, I.J., Mirza, M., Xiao, D., Courville, A., Bengio, Y.: An Empirical Investigation of Catastrophic Forgetting in Gradient-Based Neural Networks. *ArXiv e-prints* (2013). [1312.6211](https://arxiv.org/abs/1312.6211)
22. Goodfellow, I., Bengio, Y., Courville, A.: *Deep Learning*, 1st edn. MIT Press, Cambridge, MA (2016)
23. Hochreiter, S., Schmidhuber, J.: Long short-term memory. *Neural Comput.* **9**(8), 1735–1780 (1997). doi:[10.1162/neco.1997.9.8.1735](https://doi.org/10.1162/neco.1997.9.8.1735)
24. Chung, J., Gulcehre, C., Cho, K., Bengio, Y.: Empirical Evaluation of Gated Recurrent Neural Networks on Sequence Modeling. *ArXiv e-prints* (2014). [1412.3555](https://arxiv.org/abs/1412.3555)
25. SMILES. Accessed 7 April 2017. <http://www.daylight.com/dayhtml/doc/theory/theory.smiles.html>
26. Weininger, D., Weininger, A., Weininger, J.L.: Smiles. 2. algorithm for generation of unique smiles notation. *Journal of Chemical Information and Computer Sciences* **29**(2), 97–101 (1989). doi:[10.1021/ci00062a008](https://doi.org/10.1021/ci00062a008)
27. RDKit: open source cheminformatics. Version: 2016-09-3. <http://www.rdkit.org/>
28. Kingma, D.P., Ba, J.: Adam: A method for stochastic optimization. *CoRR abs/1412.6980* (2014)

29. Tensorflow. Version: 1.0.1. <http://www.tensorflow.org>
30. Williams, R.J.: Simple statistical gradient-following algorithms for connectionist reinforcement learning. *Machine Learning* **8**(3), 229–256 (1992)
31. Goodfellow, I., Pouget-Abadie, J., Mirza, M., Xu, B., Warde-Farley, D., Ozair, S., Courville, A., Bengio, Y.: Generative adversarial nets. In: *Advances in Neural Information Processing Systems*, pp. 2672–2680 (2014)
32. Lima Guimaraes, G., Sanchez-Lengeling, B., Cunha Farias, P.L., Aspuru-Guzik, A.: Objective-Reinforced Generative Adversarial Networks (ORGAN) for Sequence Generation Models. *ArXiv e-prints* (2017). [1705.10843](https://arxiv.org/abs/1705.10843)
33. Sun, J., Jeliaskova, N., Chupakin, V., Golib-Dzib, J.-F., Engkvist, O., Carlsson, L., Wegner, J., Ceulemans, H., Georgiev, I., Jeliaskov, V., Kochev, N., Ashby, T.J., Chen, H.: Escape-db: an integrated large scale dataset facilitating big data analysis in chemogenomics. *Journal of Cheminformatics* **9**(1), 17 (2017). doi:[10.1186/s13321-017-0203-5](https://doi.org/10.1186/s13321-017-0203-5)
34. Sheridan, R.P.: Time-split cross-validation as a method for estimating the goodness of prospective prediction. *J Chem Inf Model* **53**(4), 783–790 (2013)
35. Unterthiner, T., Mayr, A., Steijaert, M., Wegner, J.K., Ceulemans, H., Hochreiter, S.: Deep learning as an opportunity in virtual screening. In: *Deep Learning and Representation Learning Workshop. NIPS*, pp. 1058–1066 (2014)
36. Mayr, A., Klambauer, G., Unterthiner, T., Hochreiter, S.: Deeptox: Toxicity prediction using deep learning. *Frontiers in Environmental Science* **3**, 80 (2016)
37. Jaccard, P.: Étude comparative de la distribution florale dans une portion des Alpes et des Jura. *Bulletin de la Société Vaudoise des Sciences Naturelles* **37**, 547–579 (1901)
38. Rogers, D., Hahn, M.: Extended-connectivity fingerprints. *Journal of Chemical Information and Modeling* **50**(5), 742–754 (2010). doi:[10.1021/ci100050t](https://doi.org/10.1021/ci100050t)
39. Butina, D.: Unsupervised data base clustering based on daylight's fingerprint and tanimoto similarity: A fast and automated way to cluster small and large data sets. *Journal of Chemical Information and Computer Sciences* **39**(4), 747–750 (1999). doi:[10.1021/ci9803381](https://doi.org/10.1021/ci9803381)
40. Pedregosa, F., Varoquaux, G., Gramfort, A., Michel, V., Thirion, B., Grisel, O., Blondel, M., Prettenhofer, P., Weiss, R., Dubourg, V., Vanderplas, J., Passos, A., Cournapeau, D., Brucher, M., Perrot, M., Duchesnay, E.: Scikit-learn: Machine learning in Python. *Journal of Machine Learning Research* **12**, 2825–2830 (2011). Version 0.17
41. Silver, D., Huang, A., Maddison, C.J., Guez, A., Sifre, L., Van Den Driessche, G., Schrittwieser, J., Antonoglou, I., Panneershelvam, V., Lanctot, M., *et al.*: Mastering the game of go with deep neural networks and tree search. *Nature* **529**(7587), 484–489 (2016)
42. Reutlinger, M., Koch, C.P., Reker, D., Todoroff, N., Schneider, P., Rodrigues, T., Schneider, G.: Chemically Advanced Template Search (CATS) for Scaffold-Hopping and Prospective Target Prediction for 'Orphan' Molecules. *Mol Inform* **32**(2), 133–138 (2013)
43. Senger, S.: Using Tversky similarity searches for core hopping: finding the needles in the haystack. *J Chem Inf Model* **49**(6), 1514–1524 (2009)
44. Zaremba, W., Sutskever, I., Vinyals, O.: Recurrent neural network regularization. *CoRR abs/1409.2329* (2014)
45. Wan, L., Zeiler, M., Zhang, S., LeCun, Y., Fergus, R.: Regularization of neural networks using dropconnect. In: *Proceedings of the 30th International Conference on International Conference on Machine Learning - Volume 28. ICML'13*, pp. 1058–1066 (2013)
46. Bengio, Y., Ducharme, R., Vincent, P., Janvin, C.: A neural probabilistic language model. *J. Mach. Learn. Res.* **3**, 1137–1155 (2003)

# 1 Additional File 1.

Here is shown how the cost function of the form  $J(\theta) = [\log P(A)_{\mathbb{A}} - \log P(A)_{\mathbb{U}}]^2$  can be expressed as a REINFORCE algorithm with a single point estimate of the return  $G(a_t, s_t) = [\log P(A)_{\mathbb{A}} - \log P(A)_{\mathbb{U}}]^2 / \log P(A)_{\mathbb{A}}$ . A REINFORCE type algorithm for an episode  $\{s_0, a_0, r_0, \dots, s_T, a_T, r_T\}$  following the stochastic policy  $\pi_\theta$  is described by the update rule:

$$\theta = \theta - \alpha \nabla_\theta \sum_{t=0}^T \log \pi_\theta(a_t | s_t) (G(a_t, s_t) - b)$$

Where  $\alpha$  in this case is the step size,  $b$  is the reward baseline, and  $G(a_t, s_t) = \sum_t^T (r_t)$  is the observed cumulative reward from time  $t$  until the end of the episode. In a REINFORCE algorithm this single sampled trajectory serves as an unbiased estimator of the expected cumulative reward. If we use a zero baseline  $b = 0$ , this is equivalent to the cost function:

$$J(\theta) = \sum_{t=0}^T \log \pi_\theta(a_t | s_t) G(a_t, s_t)$$

If we define the reward for any state-action pair during the episode as equal to 0 except for the last step where it is  $G(A)$ , this expression can be written as:

$$\forall t \in [0, \dots, T], G(a_t, s_t) = \sum_t^T (r_t) = G(A)$$

The cost function becomes:

$$J(\theta) = \sum_{t=0}^T \log \pi_\theta(a_t | s_t) G(a_t, s_t) = G(A) \sum_{t=0}^T \log \pi_\theta(a_t | s_t)$$

We now note that the sum  $\sum_{t=0}^T \log \pi_\theta(a_t | s_t)$  is equal to the Agent likelihood for the sequence:

$$J(\theta) = G(A) \sum_{t=0}^T \log \pi_\theta(a_t | s_t) = G(A) \log P(A)_{\mathbb{A}}$$

If we choose the reward for the final step of the sequence  $A$  to be  $G(A) = [\log P(A)_{\mathbb{A}} - \log P(A)_{\mathbb{U}}]^2 / \log P(A)_{\mathbb{A}}$ , we recover our initial cost function:

$$J(\theta) = \frac{[\log P(A)_{\mathbb{A}} - \log P(A)_{\mathbb{U}}]^2}{\log P(A)_{\mathbb{A}}} \log P(A)_{\mathbb{A}} = [\log P(A)_{\mathbb{A}} - \log P(A)_{\mathbb{U}}]^2$$

■

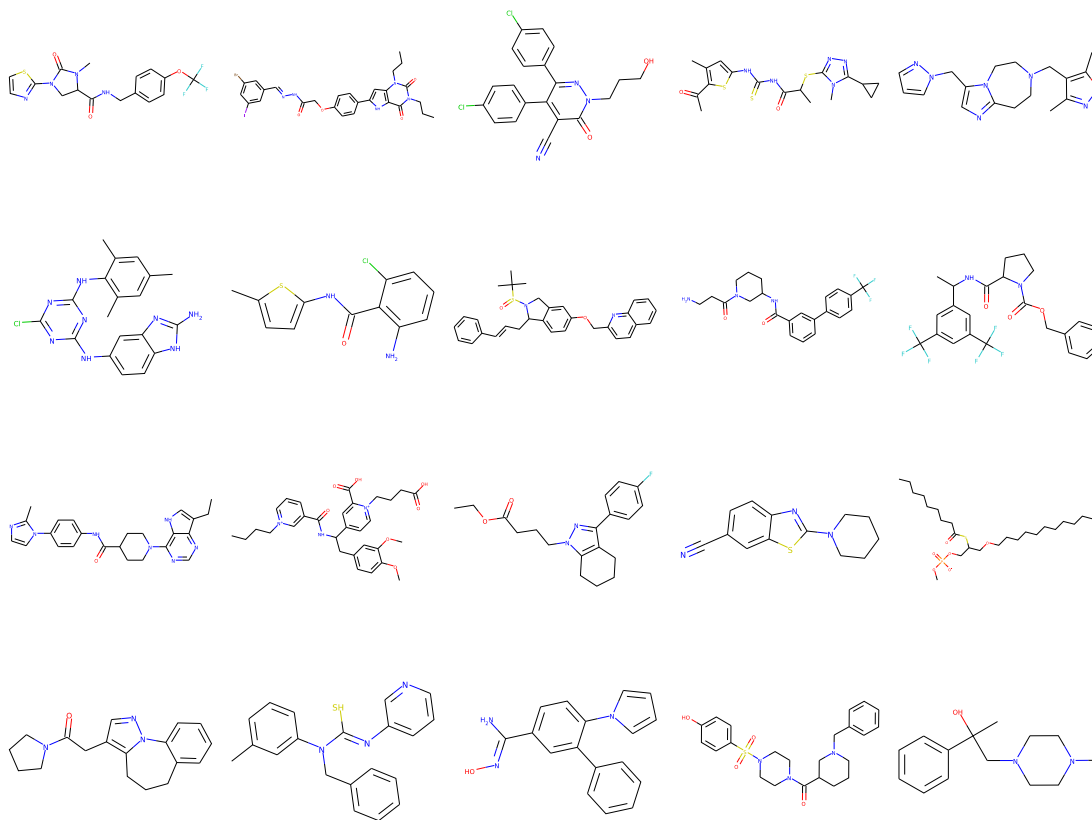


**Figure 10** Additional file 2.1 Randomly selected structures generated by the canonical Prior.

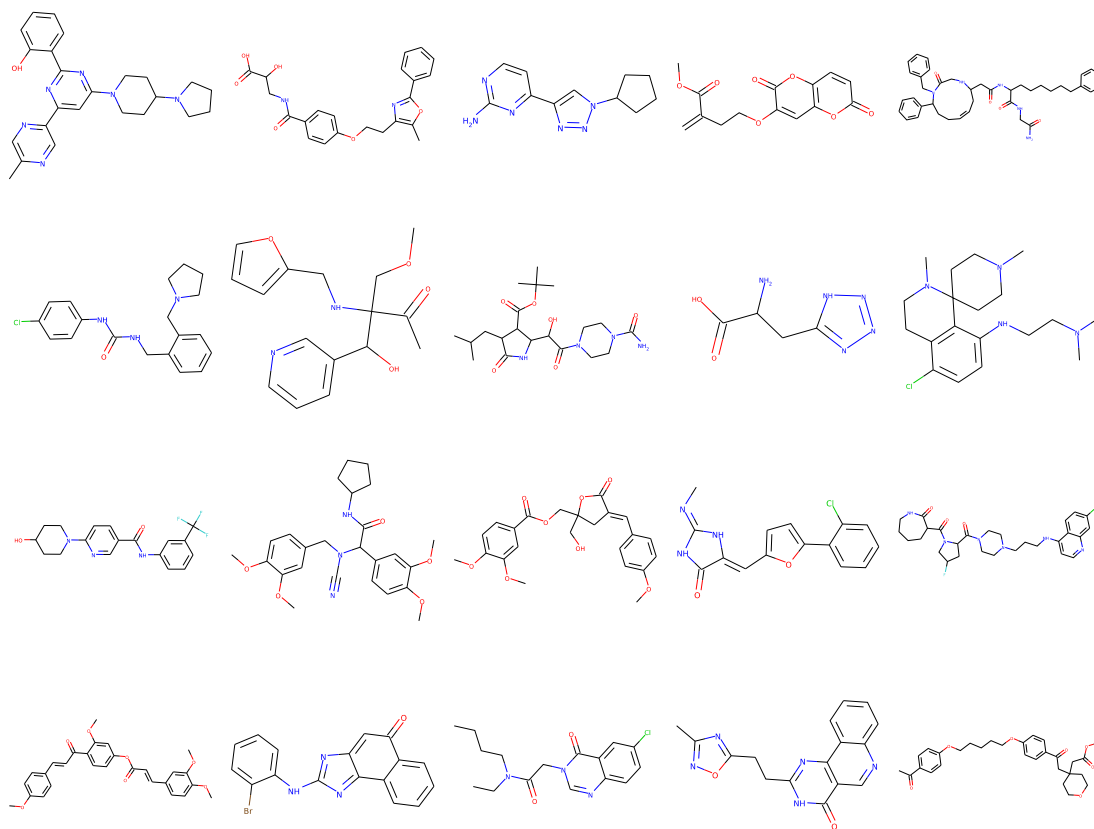


**Figure 11** Additional file 2.2 Randomly selected structures generated by the Agent trained to avoid sulphur.

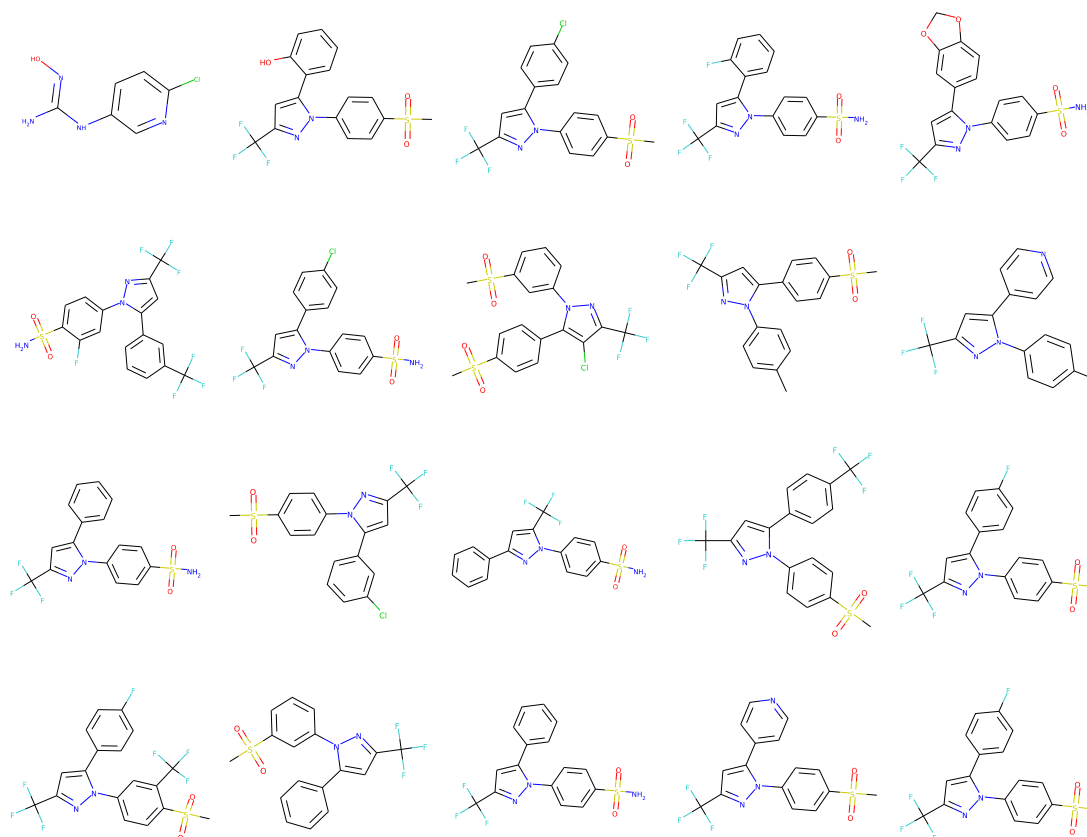


**Figure 12** Additional file 2.3 Randomly selected structures generated by the Agent based on the reduced Prior trained to design analogues of Celecoxib.

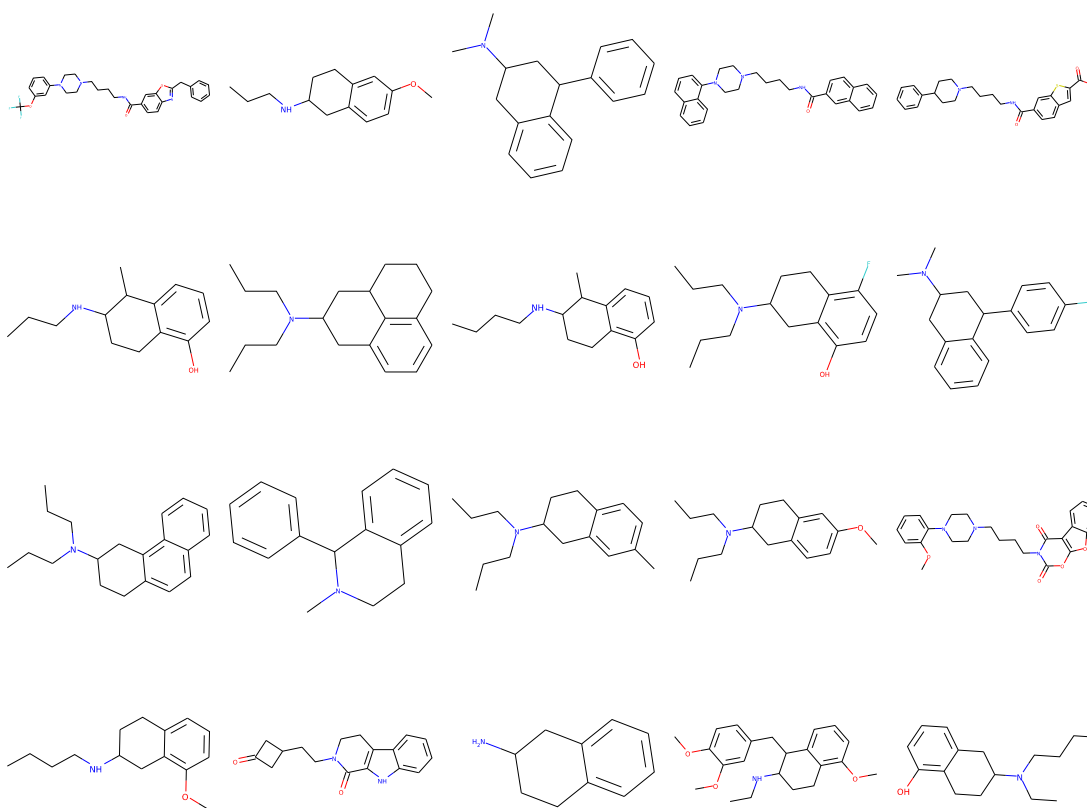


**Figure 13** Additional file 2.4 Randomly selected structures generated by the Agent based on the reduced Prior trained to design actives against DRD2.